PAPER

Effects of water on a catalytic system for preparation of N-(1,4-dimethylamyl)-N′-phenyl-p-phenylenediamine by reductive alkylation

Wenlong Yu, [ID] Junwei Ding,* Shitao Yu* and Fusheng Liu

Effects of water on a catalytic reaction system for reductive alkylation of *p*-aminodiphenylamine (*p*-ADPA) with 5-methyl-2-hexanone (MIAK) was studied. Platinum nanoparticles supported on activated carbon with high specific surface area were used as catalysts for reductive alkylation reaction under different water content conditions. Schiff base forming data, catalytic activity and stability of the catalysts were investigated under the aforementioned reaction conditions. Fresh and used catalysts were characterized by TEM, SEM, XRD, ICP, laser particle size analysis, N_2 physical adsorption and CO chemical adsorption to explore the effects of water on the catalytic reaction system for the ketone/amine reductive alkylation reaction. The characterization results indicated that catalyst support pulverization and Pt loss occurred in the reused catalyst, and the trend was more obvious under the conditions of higher water content. Water in the reaction system could also aggravate the decrease of the catalyst's specific surface area and pore volume, which should be a major reason of the lower catalytic performance.

1. Introduction

N,N′-disubstituted *p*-phenylenediamines (DPPD) play an important role in the fine chemical industry, widely used for rubber antioxidants.[1–8] As a typical kind of *N,N′*-disubstituted *p*-phenylenediamine, *N*-(1,4-dimethylamyl)-*N′*-phenyl-*p*-phenyl-enediamine (7PPD) can effectively prevent rubber from flex cracking under dynamic situations, and can be synthesized by reductive alkylation of *p*-aminodiphenylamine (*p*-ADPA) with 5-methyl-2-hexanone (MIAK).[9,10] This reaction starts with a condensation dehydration reaction between *p*-ADPA and MIAK to form a ketimine compound (Schiff base), followed by hydrogenation to 7PPD in the presence of metal catalysts.[11]

Usually, ordinary copper[12,13] and nickel based catalysts[14–16] were employed in the industrial process to manufacture DPPDs as rubber antioxidants due to their cheap costs. Unfortunately, aforementioned catalysts have obvious defects, such as low-activity and selectivity resulting in harsh reaction conditions and the ketone converting into alcohol, and copper leaching aggravating rubber aging. Precious metal[17,18] catalysts were employed to overcome the disadvantages of traditional copper-based catalysts, synthesizing DPPD compounds with high quality and efficiency.[19,20] Most of the previous work on reductive alkylation was focused on the development of catalyst with the aim of improving catalytic activity and selectivity to DPPDs.[21–24] Understanding the relationship between reaction

factors and catalytic performance, especially the effect of water generating by condensation reaction on catalytic system are of great importance considering the practical application of catalyst. Unfortunately, little effort was given to illuminate the aforementioned aspects.

In this work, the reductive alkylation reaction of *p*-ADPA with MIAK using 3 wt% Pt/AC catalyst in a refitted autoclave equipped with a hydrogen circulation machine and a ketone-water separator in order to achieve dewatering during the reaction process was investigated. A series of characterization techniques including TEM, SEM, XRD, ICP, laser particle size analysis, N_2 physical adsorption and CO chemical adsorption were applied for getting the microtopography and physico-chemical properties of the fresh and deactivated catalysts. The purpose of all the present work was to elucidate the effect of water in the reaction system on Schiff base formation and catalysts deactivation.

2. Experimental

2.1. Catalyst preparation

Pt/AC catalysts with a nominal Pt loading of 3.0 wt% were prepared by the conventional impregnation method. Prior to impregnation, a commercial activated carbon (Calgon Carbon Corp. Ltd.) was pretreated with 15% H_2O_2 at 50 °C for 5 h, followed by washing with distilled water until the pH reached 7 and then dried under vacuum at 110 °C for 12 h 15 mL of H_2PtCl_6 (Sino-Platinum Metals Corp. Ltd.) aqueous solution (0.01 g mL^{-1}) was then added dropwise into 50 mL of aqueous suspension containing 5 g of pretreated activated carbon, and

College of Chemical Engineering, Qingdao University of Science and Technology, 53 Zhengzhou Road, Qingdao 266042, People's Republic of China. E-mail: djwnsfc@ 126.com; yushitaoqust@126.com; Fax: +86 0532-84022782; Tel: +86 0532-84022782
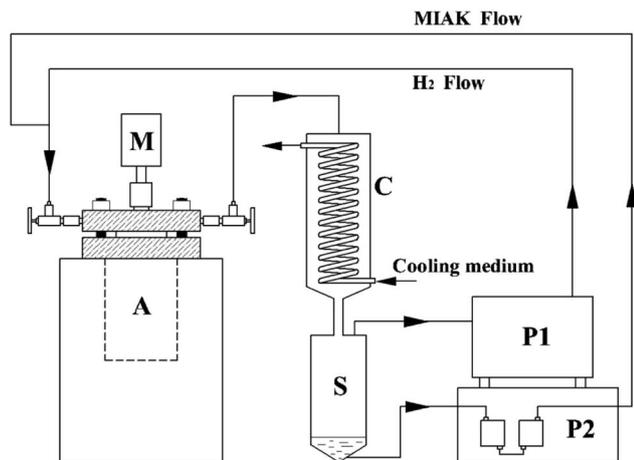
Fig. 1 Catalytic performance evaluation apparatus. A: autoclave, C: coil condenser, S: ketone–water separator, P1: hydrogen booster pump, P2: plunger pump, M: motor agitator.

then the pH of the suspension was adjusted to 10 by adding NaOH aqueous solution. The precipitated $Pt(OH)_4$ was reduced by $NaBH_4$ at room temperature, which was then washed with deionized water until the pH of the filtrate was 7 and no chloridion could be observed in the filtrate by the $AgNO_3$ titration method. This sample was then dried under vacuum at 110 °C for 12 h.

2.2. Evaluation reaction

The condensation and reductive alkylation as evaluation reactions were conducted in an autoclave (Weihai Huixin Chemical Mechanic Corp. Ltd.) which was made of stainless steel with a working volume of 500 mL. The autoclave was refitted which was equipped with a hydrogen circulation machine (Zhejiang SMT Technology Corp. Ltd.), a coil condenser with ketone–water separator and a plunger pump in order to dewater continuously and achieve the circulation of hydrogen and MIAK condensed (Fig. 1).

The condensation reaction conditions were as follows: p-ADPA = 50 g, MIAK = 120 g, Pt/AC = 0.5 g, $T = 373$ K, $P = 3.0$ MPa (pure N_2), stirring speed = 600 rpm. The reductive

alkylation reactions were performed in the same conditions except for replacing N_2 with pure H_2. All the reactions were carried out in normal mode, adding water and dewatering condition respectively, in order to investigate the effects of water content on the reaction results. 10 g of H_2O was added in adding water mode while H_2O generating during condensation reaction was removed with H_2 and MIAK steam in dewatering condition. H_2 and MIAK condensed were returned to the autoclave depend on the hydrogen circulation machine and plunger pump. The catalyst was recycled by filtration after reaction. The reaction products were analyzed by gas chromatography (Agilent 7820A) equipped with an FID detector and a capillary column HP-5 (0.32 mm × 30 m).

The conversion of p-ADPA and selectivity of 7PPD can be calculated by the following equations respectively:

$$X = \frac{C^0_{p\text{-ADPA}} - C_{p\text{-ADPA}}}{C^0_{p\text{-ADPA}}} \times 100\% \qquad (1)$$

$$S = \frac{C_{7PPD}}{C^0_{p\text{-ADPA}} - C_{p\text{-ADPA}}} \times 100\% \qquad (2)$$

where X is the p-ADPA conversion, S is the 7PPD selectivity, C^0 and C denote the initial and final mole fraction, respectively.

2.3. Catalyst characterization

Scanning electron microscopy (SEM) was performed on a JSM-7500F microscope (JEOL Ltd.) with an accelerating voltage of 8.0 kV. The samples were then gold coated by cathodic sputtering. Transmission electron microscopy (TEM) images of the catalysts were obtained using a JEM-2100F microscope (JEOL Ltd.) operating at an accelerating voltage of 200 kV. The samples for TEM were prepared by dropping the ethanol suspensions of the catalysts on copper grids. The powder X-ray diffraction (XRD) patterns of the samples were recorded on D/max 2500 diffractometer with Cu K_α radiation at 40 kV and 150 mA. The Pt content of the catalysts were quantitatively determined by inductively coupled plasma atomic emission spectroscopy (ICP-AES) using a Varian715-ES. The particle sizes of the catalysts were determined using a Mastersizer 3000 laser particle size
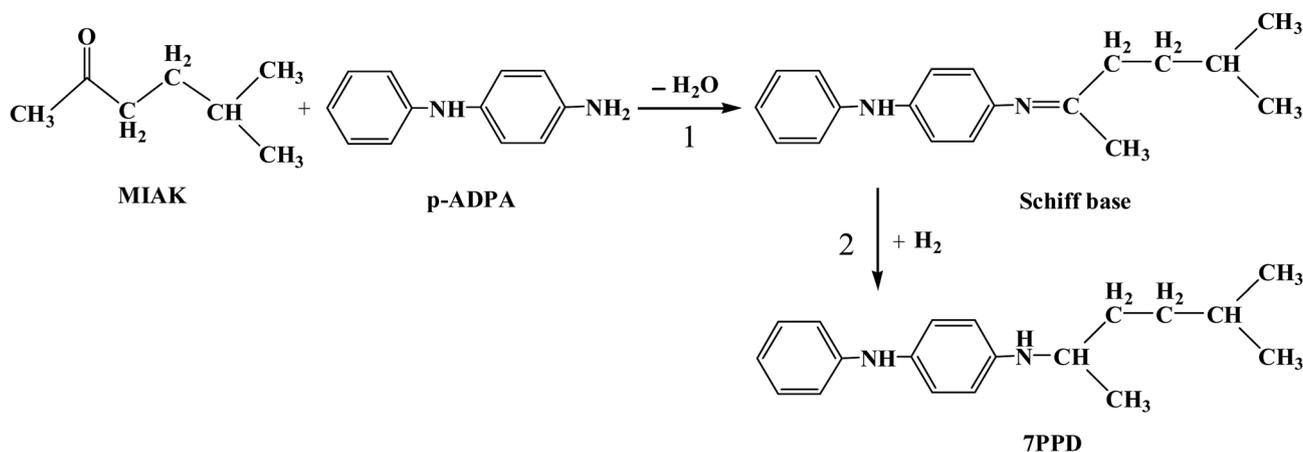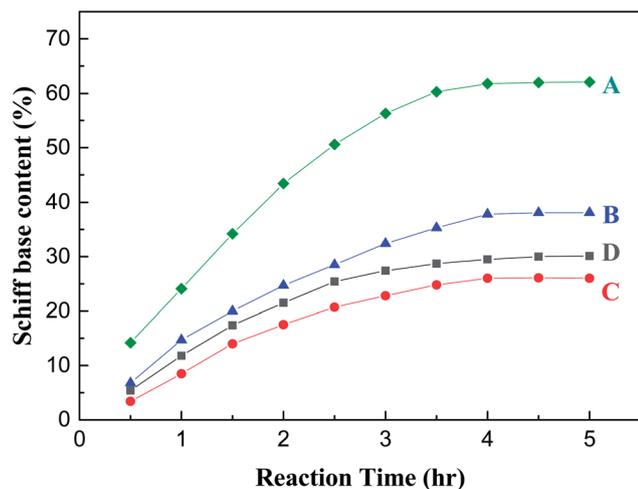

Scheme 1 Reaction pathways.

Fig. 2 Time on Schiff base generation over Pt/AC in dewatering (A), normal (B) and adding water (C) conditions respectively. Blank experiment: Schiff base generation without any catalysts in normal reaction mode (D). Reaction condition: p-ADPA = 50 g, MIAK = 120 g, Pt/AC = 0.5 g, T = 373 K, P = 3.0 MPa (pure N_2), stirring speed = 600 rpm.

analyzer (Malvern Panalytical Corp.). The surface area and pore structure of the catalysts were determined by N_2 physical adsorption using a ASAP 2020 surface area analyzer (Micromeritics Instrument Corp.). The surface area of the samples was calculated by the BET equation. The specific surface area of Pt supported on the activated carbon was determined by CO chemical adsorption using a AutoChemII 2920 analyzer (Micromeritics Instrument Corp.).

3.   Results and discussion

3.1.   Evaluation reaction results

In order to elucidate the effects of water content on the reaction results, the condensation reaction and reductive alkylation reaction of p-ADPA with MIAK were investigated in normal mode, adding water and dewatering condition, respectively. The reaction for the synthesis of N-(1,4-dimethylamyl)-N′-phenyl-p-phenylenediamine (7PPD) is shown in Scheme 1. For the condensation of p-ADPA with MIAK, as shown in Fig. 2, in the normal reaction mode, the equilibrium generation of Schiff base was 38%, and the reaction reached equilibrium at 4 h. When additional water was added in the reaction system, the

Table 1 Catalytic performance of Pt/AC catalysts in the synthesis of 7PPD

Reaction mode[a]	Reaction time/hr	p-ADPA conversion/%	7PPD selectivity/%
Blank experiment[b]	4.5	30	0
Normal condition	5	100	96.4
H_2O added condition	8	85	82.4
Dewatering condition	2.5	100	99.4

[a] Reaction condition: p-ADPA = 50 g, MIAK = 120 g, Pt/AC = 0.5 g, T = 373 K, P = 3.0 MPa (pure H_2), stirring speed = 600 rpm. [b] Blank experiment was carried out without any catalysts in normal reaction mode.

formation rate of Schiff base slowed down with the equilibrium generation of Schiff base reducing to 26%. Under the condition of continuous dewatering, a significant increase of the Schiff base formation rate was attained, with the equilibrium generation of Schiff base rising to 62%. In the normal reaction mode, the equilibrium generation of Schiff base was 30% without any catalysts, and the reaction reached equilibrium at 4.5 h. The reason why both the formation rate and equilibrium generation of Schiff base were a little higher in presence of the catalyst may be due to catalysis of activated carbon to the condensation reaction. The formation rate and equilibrium generation of Schiff base were influenced by the water content of the reaction system based on the principle of chemical equilibrium. The condensation of p-ADPA with MIAK could be promoted due to removing water in time.

For the reductive alkylation of p-ADPA with MIAK in the presence of hydrogen, as shown in Table 1, p-ADPA was completely converted in 5 h with a selectivity (96.4%) obtained under the normal reaction condition. When additional H_2O was added in the reaction system, the reaction time was extended to 8 h with a lower conversion of p-ADPA (85%) and a lower selectivity (82.4%) to 7PPD. In contrast, both a high selectivity (99.4%) and a shorter reaction time (2.5 h) could be obtained with a complete conversion of p-ADPA under the condition of continuous dewatering. It could be inferred that the formation rate of Schiff base was slowed down due to the increase of water content in the reaction system which caused a mismatch between Schiff base generating and hydrogenation. The side reactions might be aggravated due to the imbalance of two-step reactions which led to a lower selectivity of 7PPD.

The initial water content in adding water, normal mode and dewatering condition were 5.6 wt%, 0 wt% and 0 wt%, respectively. The water content increased constantly with the condensation dehydration reaction between p-ADPA and MIAK carrying out in adding water and normal condition, while
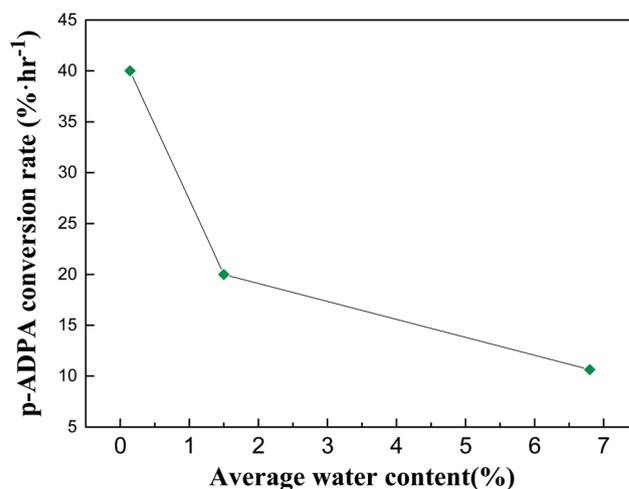

Fig. 3 Relationship between catalytic activity and water content. P-ADPA conversion rate was calculated by the following equation: $W = \frac{X_{p\text{-ADPA}}}{t}$, where W is the p-ADPA conversion rate, X is the p-ADPA conversion, t is the reaction time.
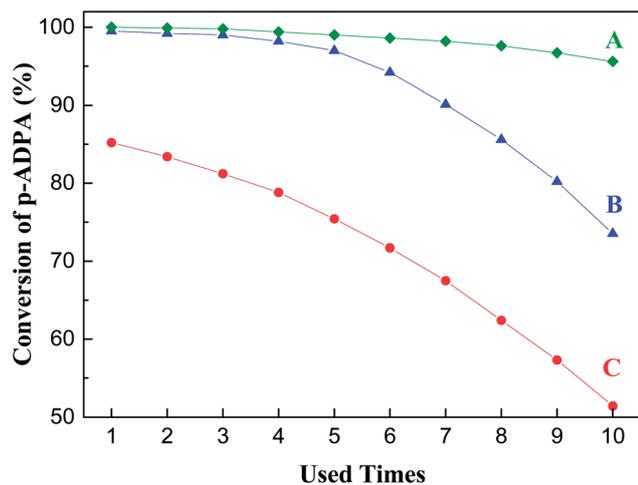
Fig. 4 Recyclability of Pt/AC for reductive alkylation in dewatering (A), normal (B) and adding water (C) conditions respectively. Reaction condition: p-ADPA = 50 g, MIAK = 120 g, Pt/AC = 0.5 g, T = 373 K, P = 3.0 MPa (pure H_2), stirring speed = 600 rpm.

almost all the water generating could be removed from the reaction system under dewatering condition. The final water content calculated in adding water, normal mode and dewatering condition were 7.9 wt%, 2.9 wt% and 0.18 wt%, respectively, according to the conversion of p-ADPA and quantity of water removed (4.6 g). Fig. 3 presents the relationship between catalytic activity and water content. Average water content can be calculated to estimate the water content during the reaction process (6.8 wt%, 1.5 wt% and 0.14 wt% in adding water, normal mode

and dewatering condition, respectively). It was obvious that the p-ADPA conversion rate reduced sharply with the increase of average water content in the reaction system.

The stability of catalysts in reductive alkylation reactions of p-ADPA with MIAK was investigated *via* the reuse of catalysts under the same reaction conditions as mentioned above. As shown in Fig. 4, under the dewatering condition, the p-ADPA conversion remained above 95% after the catalyst reused 10 times. However, significant decrease of p-ADPA was obtained under the normal and additional water added conditions with the increase of catalysts reused times, which might be inferred some relations between the catalyst deactivation and the water content of the reaction system.

3.2. Catalyst characterization

The fresh catalyst (F) and catalysts reused 10 times in dewatering (A), normal (B), and adding water (C) conditions respectively were characterized. To explore the surface structure and morphology of fresh and used catalysts, SEM characterization was carried out, as shown in Fig. 5. It was observed that carbon supports of fresh and reused catalyst under the dewatering condition had large particle structure, while the supports of catalysts reused under the normal and additional water added conditions had become broken somewhat. Water of the reaction system might aggravate the crush of carbon supports which might do damage to the pore structure or cause filtration loss of the catalysts.

The TEM images of fresh and used catalysts are given in Fig. 6. It was noted that the highly dispersed Pt nanoparticles,
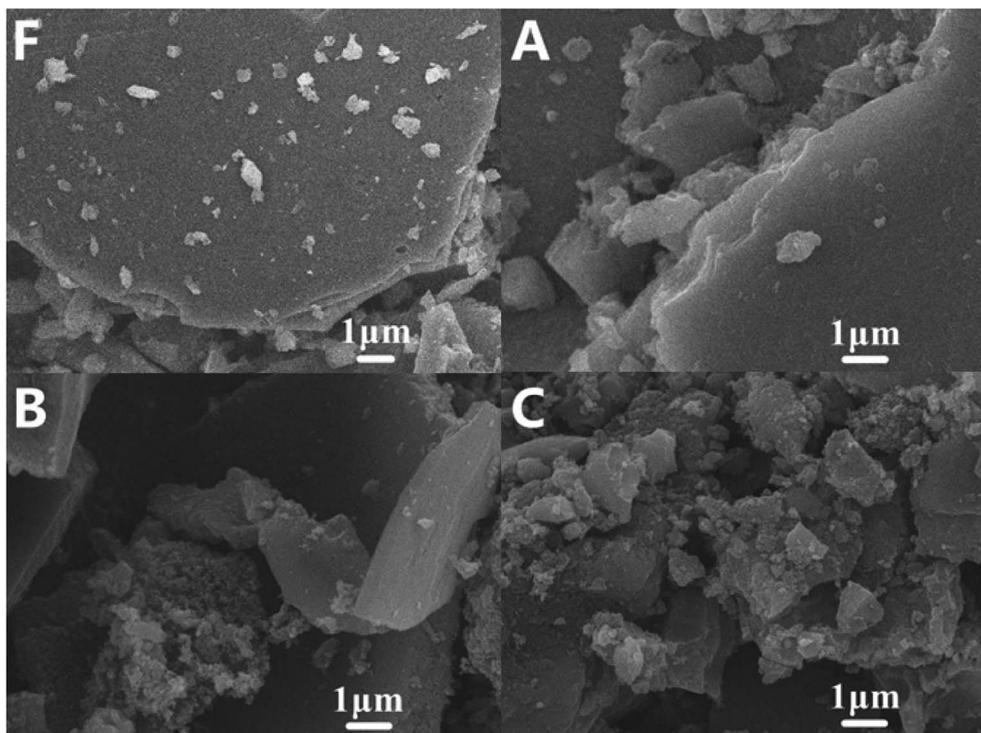

Fig. 5 SEM images of fresh Pt/AC (F), Pt/AC reused in dewatering condition (A), Pt/AC reused in normal condition (B), Pt/AC reused in adding water condition (C).
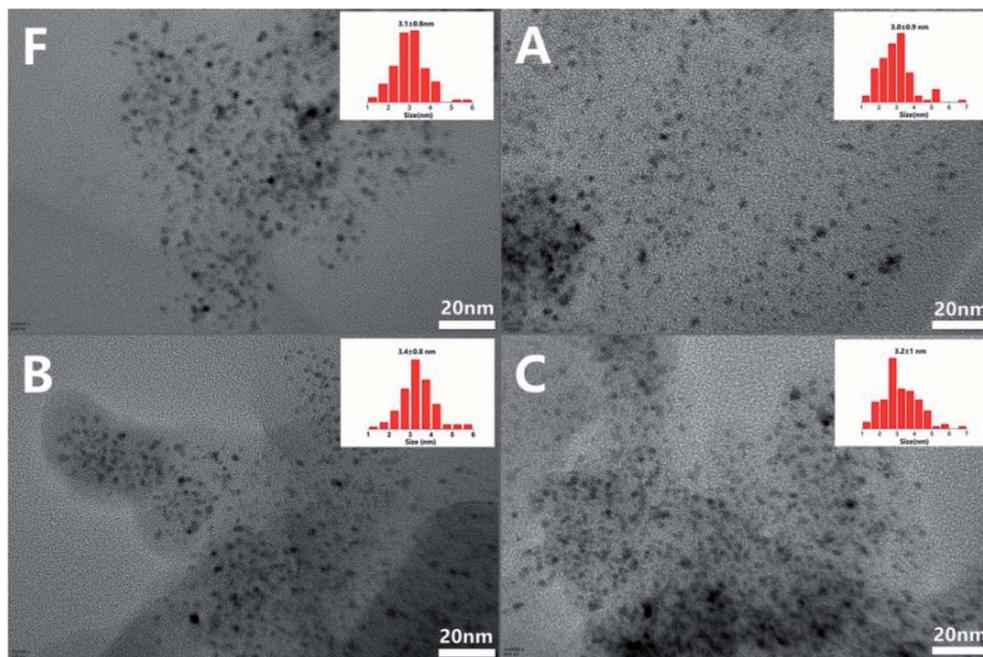
Fig. 6 TEM images and particle size distribution of fresh Pt/AC (F), Pt/AC reused in dewatering condition(A), Pt/AC reused in normal condition (B), Pt/AC reused in adding water condition(C).

2–4 nm in size, were uniformly distributed within the supports and no obvious nanoparticles aggregation was observed in fresh catalyst as well as catalysts reused under the different conditions. The results revealed that the effect of water on the dispersion of Pt nanoparticles was slight which might benefit from the mild reductive alkylation reaction conditions ($T = 373$ K, H_2 $P = 3.0$ MPa).

Fig. 7 presents the XRD patterns of fresh and used catalysts. Usually, the diffraction peaks of Pt in Pt/AC are weak and obscured in the XRD patterns, indicating the successful formation of well-dispersed ultrasmall Pt nanoclusters on the supports. It was obvious that all the catalysts had only broad diffraction peak at $2\theta = 25°$ attributed to the amorphous carbon and no characteristic diffraction peaks of Pt were found, which was possibly due to Pt nanoparticles being completely highly dispersed and there were no obvious changes of Pt crystalline state in catalysts reused process under the different conditions. This result is in accordance with the conclusion of TEM analysis.

Pt content and average particle size of fresh and used catalysts are presented in Table 2. The Pt content of fresh catalyst was about 2.91 wt%, while Pt loss was more serious with the increase of water content in the reaction system for catalysts reused under the different conditions. Considering the changes of catalyst powders average particle size and SEM analysis, the reason for the loss of Pt was likely to be filtration loss caused by the crushing of catalyst supports.

Furthermore, N_2 physical adsorption and CO chemical adsorption characterization of fresh and used catalysts were carried out. It is evident from Table 3 that the BET specific surface area and pore volume of used catalysts all decreased comparing with fresh catalyst, and the trend was more obvious
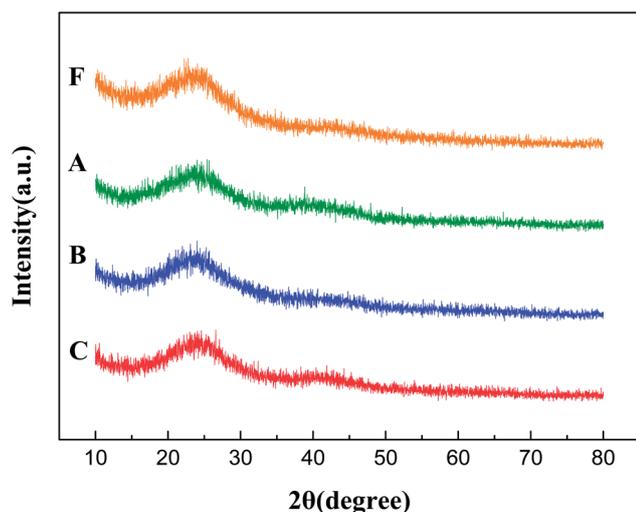

Fig. 7 XRD patterns of fresh Pt/AC (F), Pt/AC reused in dewatering condition (A), Pt/AC reused in normal condition (B), Pt/AC reused in adding water condition (C).

Table 2 Pt content and average particle size of fresh and used catalysts

Catalyst samples	Pt content/%	Average particle size/mesh
Fresh catalyst	2.91	360
Catalyst reused in dewatering condition	2.85	370
Catalyst reused in normal condition	2.74	410
Catalyst reused in H_2O added condition	2.52	480

Table 3 Textural properties of the fresh and used catalysts

Catalyst samples	$S_{BET}/m^2 g^{-1}$	$V_{total}/cm^3 g^{-1}$	Pore size/nm	$S_{Pt}/m^2 g^{-1}$
Fresh catalyst	1312.62	1.17	4.20	48.51
Catalyst reused in dewatering condition	978.42	0.91	4.32	36.63
Catalyst reused in normal condition	628.41	0.62	4.63	21.66
Catalyst reused in H$_2$O added condition	514.13	0.43	4.87	7.18

under the condition of higher water content. Corresponding, Pt specific surface area of used catalysts had a similar trend. These results suggested that higher water content in the reaction system aggravated the deteriorating of catalysts surface structure. According to the results of catalyst characterization and evaluation reaction, it can be concluded, during the reductive alkylation of *p*-ADPA with MIAK over Pt/AC under the condition of high water content, some organics generating by side reactions would adsorb on the catalyst, and these organics could block pores and cover active centers, leading to the decrease in the surface area and catalytic activity.

4. Conclusions

Effects of water in the reaction system on reductive alkylation of *p*-ADPA with MIAK and Pt/AC catalysts deactivation were investigated in normal mode, adding water and dewatering condition, respectively. Water in the reaction system could decrease the formation rate of Schiff base and the conversion of *p*-ADPA, as well as the selectivity of 7PPD and the stability of catalysts. Catalyst characterization results reflected that catalyst supports pulverization and Pt loss occurred in catalysts reused, and the trend was more obvious under the condition of higher water content. Water in the reaction system also aggravated the decrease of catalysts specific surface area and pore volume, which should be a major reason of lower catalytic performance. This work demonstrated that it was essential to control the water content of reductive alkylation.

Conflicts of interest

There are no conflicts to declare.

Acknowledgements

References

1 F. Cataldo, *Eur. Polym. J.*, 2002, **38**, 885–893.

2 F. Cataldo, *Polym. Degrad. Stab.*, 2018, **147**, 132–141.

3 Z. Cibulková, P. Šimon, P. Lehocký and J. Balko, *Polym. Degrad. Stab.*, 2005, **87**, 479–486.

4 I. Puškárová, M. Šoral and M. Breza, *Chem. Phys. Lett.*, 2015, **639**, 78–82.

5 P. Rapta, A. Vargová, J. Polovková, A. Gatial, L. Omelka, P. Majzlík and M. Breza, *Polym. Degrad. Stab.*, 2009, **94**, 1457–1466.

6 I. Puškárová and M. Breza, *Polym. Degrad. Stab.*, 2016, **128**, 15–21.

7 A. V. Babkin, A. F. Asachenko, D. V. Uborsky, D. S. Kononovich, V. V. Izmer, V. A. Kudakina, V. A. Shnaider, N. E. Shevchenko and A. Z. Voskoboynikov, *Mendeleev Commun.*, 2016, **26**, 555–557.

8 A. Gatial, J. Polovková, I. Kortišová and M. Breza, *Vib. Spectrosc.*, 2007, **44**, 1–8.

9 H. L. Merten and L. M. Baclawski, *US Pat.*, 4900868, 1990.

10 R. M. DSidocky and D. K. Parker, *US Pat.*, 4463191, 1984.

11 M. A. Fox and J. K. Whitesell, *Organic Chemistry*, Jones and Bartlett Publishers, Boston, MA, 1994, p.72.

12 M. J. Zhang, D. W. Tan, H. X. Li, D. J. Young, H. F. Wang, H. Y. Li and J. P. Lang, *J. Org. Chem.*, 2018, **83**, 1204–1215.

13 D. W. Tan, H. X. Li, D. L. Zhu, H. Y. Li, D. J. Young, J. L. Yao and J. P. Lang, *Org. Lett.*, 2018, **20**, 608–611.

14 S. Ward, S. A. Lamb and M. A. E. Hodgson, *British Pat.*, 712100, 1951.

15 Y. Z. Zhang and Q. Wei, *CN Pat.*, 1370748, 2002.

16 H. V. Bramer, L. G. Davy and M. L. Clemens, *US Pat.*, 2323948, 1943.

17 S. Y. Liu, L. Y. Xu, C. Y. Liu, Z. G. Ren, D. J. Young and J. P. Lang, *Tetrahedron*, 2017, **73**, 2374–2381.

18 T. Y. Feng, H. X. Li, D. J. Young and J. P. Lang, *J. Org. Chem.*, 2017, **82**, 4113–4120.

19 F. N. Schwettmann, *US Pat.*, 3384664, 1968.

20 K. Tada, N. Kodear, M. Hanai and K. Hirabayashi, *JP Pat.*, 82123148, 1982.

21 Q. F. Zhang, F. Feng, C. Su, W. Xu, L. Ma, C. S. Lu and X. N. Li, *RSC Adv.*, 2015, **5**, 66278–66285.

22 W. Xu, J. Ni, Q. F. Zhang, F. Feng, Y. Z. Xiang and X. N. Li, *J. Mater. Chem. A*, 2013, **1**, 12811–12817.

23 Q. F. Zhang, J. C. Wu, C. Su, F. Feng, Q. L. Ding, Z. L. Yuan, H. Wang, L. Ma, C. S. Lu and X. N. Li, *Chin. Chem. Lett.*, 2012, **23**, 1111–1114.

24 N. G. Patil, D. Roy, A. S. Chaudhari and R. V. Chaudhari, *Ind. Eng. Chem. Res.*, 2007, **46**, 3243–3254.